



# Characterization of conformational deformation-coupled interaction between immunoglobulin G1 Fc glycoprotein and a low-affinity Fc $\gamma$ receptor by deuteration-assisted small-angle neutron scattering<sup>☆</sup>



Rina Yogo<sup>a,b</sup>, Saeko Yanaka<sup>a,b</sup>, Hirokazu Yagi<sup>b</sup>, Anne Martel<sup>c</sup>, Linoel Porcar<sup>c</sup>, Yutaro Ueki<sup>d</sup>, Rintaro Inoue<sup>e</sup>, Nobuhiro Sato<sup>e</sup>, Masaaki Sugiyama<sup>e,\*</sup>, Koichi Kato<sup>a,b,\*\*</sup>

<sup>a</sup> Okazaki Institute for Integrative Bioscience and Institute for Molecular Science, National Institutes of Natural Sciences, 5-1 Higashiyama, Myodaiji, Okazaki, Aichi 444-8787, Japan

<sup>b</sup> Graduate School of Pharmaceutical Sciences, Nagoya City University, 3-1 Tanabe-dori, Mizuhoku, Nagoya 467-8603, Japan

<sup>c</sup> Institut Laue-Langevin, 6 Rue Jules Horowitz, Grenoble 38042, France

<sup>d</sup> Graduate School of Engineering, Kyoto University, Yoshida-honmachi, Sakyo-ku, Kyoto 606-8501, Japan

<sup>e</sup> Research Reactor Institute, Kyoto University, Kumatori, Sennan-gun, Osaka 590-0494, Japan

## A B S T R A C T

A recently developed integrative approach combining varied types of experimental data has been successfully applied to three-dimensional modelling of larger biomacromolecular complexes. Deuteration-assisted small-angle neutron scattering (SANS) plays a unique role in this approach by making it possible to observe selected components in the complex. It enables integrative modelling of biomolecular complexes based on building-block structures typically provided by X-ray crystallography. In this integrative approach, it is important to be aware of the flexible properties of the individual building blocks. Here we examine the ability of SANS to detect a subtle conformational change of a multidomain protein using the Fc portion of human immunoglobulin G (IgG) interacting with a soluble form of the low-affinity Fc $\gamma$  receptor IIIb (sFc $\gamma$ RIIIb) as a model system. The IgG-Fc glycoprotein was subjected to SANS in the absence and presence of 75%-deuterated sFc $\gamma$ RIIIb, which was matched out in D<sub>2</sub>O solution. This inverse contrast-matching technique enabled selective observation of SANS from IgG-Fc, thereby detecting its subtle structural deformation induced by the receptor binding. The SANS data were successfully interpreted by considering previously reported crystallographic data and an equilibrium between free and sFc $\gamma$ RIIIb-bound forms. Our SANS data thus demonstrate the applicability of SANS in the integrative approach dealing with biomacromolecular complexes composed of weakly associated building blocks with conformational plasticity.

## 1. Introduction

Recent progress in X-ray crystallography has yielded more than hundred thousand protein structures deposited in the Protein Data Bank. As such, current trends in structural biology are increasingly focusing on more complicated macromolecular complexes, which remain difficult to analyze using traditional approaches. A recently developed approach for dealing with such complex and often huge systems is integrating the atomic coordinates of individual building blocks

determined by X-ray crystallography and/or NMR spectroscopy into a low-resolution three-dimensional (3D) map as a template provided typically by cryo-electron microscopy [1]. This integrative approach has successfully resulted in 3D structure models of biomolecular assemblies such as HIV capsid assemblies and the DNA telomerase complex [2,3].

Solution scattering also provides information on gross shapes of biomacromolecular complexes complemented by crystal structures. In particular, small-angle neutron scattering (SANS) enables selective observation of specific components in the complexes by selective

<sup>☆</sup> **Synopsis:** Our inverse contrast-matching technique enabled the selective observation of small-angle neutron scattering of human immunoglobulin G1 Fc glycoprotein in complex with its cognate receptor. Using this method, the receptor-induced quaternary structure deformation of the glycoprotein was detected under equilibrium between its free and receptor-bound forms.

\* Corresponding author.

\*\* Corresponding author at: Okazaki Institute for Integrative Bioscience and Institute for Molecular Science, National Institutes of Natural Sciences, 5-1 Higashiyama, Myodaiji, Okazaki, Aichi 444-8787, Japan.

E-mail addresses: [sugiyama@rii.kyoto-u.ac.jp](mailto:sugiyama@rii.kyoto-u.ac.jp) (M. Sugiyama), [kkatonmr@ims.ac.jp](mailto:kkatonmr@ims.ac.jp) (K. Kato).

<http://dx.doi.org/10.1016/j.bbrep.2017.08.004>

Received 29 April 2017; Received in revised form 20 July 2017; Accepted 10 August 2017

Available online 16 August 2017

2405-5808/ © 2017 The Authors. Published by Elsevier B.V. This is an open access article under the CC BY-NC-ND license (<http://creativecommons.org/licenses/by-nc-nd/4.0/>).

deuteration combined with contrast-matching methods. This is because the neutron scattering length is different between hydrogen and deuterium. This technique was pioneeringly applied to determine the spatial arrangements of 30 S ribosomal subunits [4] and recently sophisticated as exemplified by the application to quaternary structure analyses of a variety of protein complexes [5–8]. Deuteration-assisted SANS data in conjunction with crystallographic data has thus facilitated 3D modelling of quaternary structure views of protein complexes like the circadian clock protein complex, KaiB and KaiC [9], and the large dodecameric aminopeptidase TET [10].

In this integrative approach, it is important to correctly assess the conformational alteration of each component upon complex formation, when the overall complex structures are fabricated with the individual building-block structures. It is generally difficult to integrate flexible parts of the building blocks, whose electron densities are often missing in the crystal structure [6,11–13]. This is particularly problematic if the subunits are modified with flexible oligosaccharide moieties. Furthermore, if some building blocks were assembled through weak interactions, dynamic equilibrium between complexed and uncomplexed states should be considered to accurately interpret the data.

In view of this situation, we examined the capability of SANS to deal with protein complexes involving glycoproteins that undergo conformational alteration upon their weak association. As a model system, we used an interaction between the Fc region of human IgG1 (IgG1-Fc) and a low-affinity Fc $\gamma$  receptor (Fc $\gamma$ R), Fc $\gamma$ RIIIb. IgG1-Fc consists of two identical 26 kDa-polypeptide chains each divided into C<sub>H</sub>2 and C<sub>H</sub>3 domains. Each C<sub>H</sub>2 domain possesses a conserved glycosylation site at Asn297 displaying a complex-type oligosaccharide (with a molecular mass of 1.6 kDa), which is indispensable for binding to Fc $\gamma$ Rs including Fc $\gamma$ RIIIb. Several crystal structures have been reported for human IgG1-Fc in uncomplexed and complexed with a soluble form of Fc $\gamma$ RIIIb (sFc $\gamma$ RIIIb), composed of the extracellular domains (with a molecular mass of 21.4 kDa), indicating a conformational change of Fc upon formation of their 1:1 complex (Fig. 1). This allows us to assess the capability of the deuteration-assisted SANS method to detect conformational alterations of the multidomain glycoprotein in solution upon interacting with its low-affinity binding partner.

## 2. Materials and methods

### 2.1. Protein preparation

The Fc fragments were prepared by papain digestion from human IgG1. The extracellular regions of human Fc $\gamma$ RIIIb was expressed using *Escherichia coli* strain BL21(DE3) as inclusion body. For preparation of deuterated proteins, the bacterial cells were grown in an M9 minimal

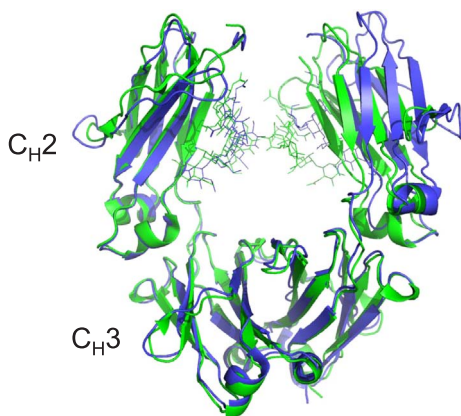


Fig. 1. Superposition of crystal structures of Fc in free (PDB code 3AVE, green) and sFc $\gamma$ RIIIb-bound states (PDB code 1T89, blue). The carbohydrate moieties are displayed in wireframe model.

medium containing 2 g/l of glucose as a 1–3 mixture of isotopically natural and fully deuterated glucose (1,2,3,4,5,6,6-D<sub>7</sub>, 98%, Cambridge Isotope Laboratories Inc.), along with a 25:75 ratio of H<sub>2</sub>O and D<sub>2</sub>O as previously described [6]. The inclusion body was suspended in 50 mM Tris-HCl, pH 8.0, containing 150 mM NaCl. After sonication, the homogenate was centrifuged at 8000g for 15 min at 4 °C and the precipitate was denatured by 8 M urea. The denatured protein solution was diluted with refolding buffer (50 mM Tris-HCl, pH 8.0, 0.5 M arginine, 5 mM CaCl<sub>2</sub>, 5 mM reduced form of glutathione, and 0.5 mM oxidized form of glutathione). After two days of incubation at 4 °C, the diluted protein solution was applied to cComplete His-Tag Purification Resin (Roche) and further purified on the HiLoad 26/60 Superdex 75 pg column (GE Healthcare).

### 2.2. Solution scattering measurements

SANS experiments were performed using the D22 instrument installed at the Institut Laue-Langevin (ILL), Grenoble, France (Table S1). The SANS intensities were observed with 6.0 Å neutrons and two sample-to-detector distances of 5.6 m and 1.4 m: the covered  $q$ -ranges are 0.01–0.55 Å<sup>-1</sup>. The temperature was maintained at 25 °C in the irradiation. The observed SANS intensity was corrected for background, empty cell and buffer scatterings, and transmission factors and subsequently converted to the absolute scale by GRASP software using incident beam flux (<http://www.ill.eu/instruments-support/instruments-groups/groups/lss/grasp/home/>).

For all SANS measurements, we used 99.8% D<sub>2</sub>O (ISOTEC) containing 50 mM Tris-HCl, pH 8.0, and 150 mM NaCl as the solvent to reduce the incoherent scattering and obtain high statistical data in the higher  $q$ -range. We measured the SANS of non-deuterated Fc (14 μM, 0.73 mg/ml) and 75%-deuterated sFc $\gamma$ RIIIb (31 μM, 0.70 mg/ml) as well as their 1:1 mixture at each concentration of 16 μM (0.83 mg/ml of Fc plus 0.36 mg/ml of sFc $\gamma$ RIIIb). As reference, 75%-deuterated sFc $\gamma$ RIIIb (31 μM) under identical solution conditions was also subjected to small-angle X-ray scattering (SAXS) measurement with BL15A2 at Photon Factory, KEK, Tsukuba, Japan.

SANS profiles were calculated from atomic coordinates deposited in the Protein Data Bank (PDB) with Debye functions, taking into account the deuteration ratios of both solvent-exchangeable and nonexchangeable hydrogens, as well as the excluding volume of the protein(s) (Table S2) (for more detail, refer to Supplementary Method in Supplementary Materials).

## 3. Results and discussions

In this study, we performed SANS characterization of human IgG1-Fc in solution in both the presence and absence of sFc $\gamma$ RIIIb. Firstly, we observed a SANS profile of human IgG-Fc alone, which was compared with theoretical profiles computed from its crystal structure (Fig. 2). The observed profile was well reproduced by the simulated curve only when the carbohydrate moieties attached to Fc were considered in the calculation.

Because the total contrast and scattering intensity of the carbohydrate part are much smaller than those of the polypeptide part in IgG1-Fc (Fig. S1 (a) and (b)), it is expected that the glycans contribute only very slightly to the scattering profiles. However, our simulation based on the crystal structure indicates that the glycans specifically affected the scattering profile in the  $q$ -range of 0.12–0.20 Å<sup>-1</sup>, where the interference term between the glycans and the polypeptides in Fc was specifically negative (Fig. S1 (c)). This  $q$ -dependent effect can be attributed to the unique horseshoe-shaped structure of Fc accommodating the glycans in its cavity (Fig. 1). The experimentally obtained SANS profile can be thus interpreted, confirming that the pair of biantennary complex-type oligosaccharides are packed between the two C<sub>H</sub>2 domains as observed in the crystal structure.

Next, we observed SANS profiles of IgG1-Fc in complex with

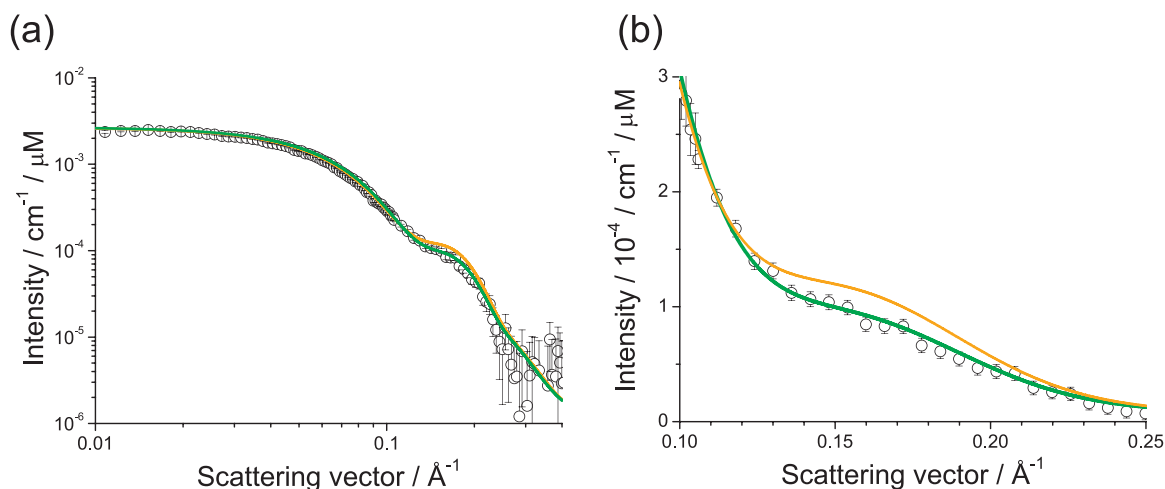


Fig. 2. (a) SANS profile for Fc alone (open circles) shown with theoretical profiles computed from the crystal structure of human IgG1-Fc in an uncomplexed state with (green) and without (orange) the glycan parts. (b) The enlarged view of (a).

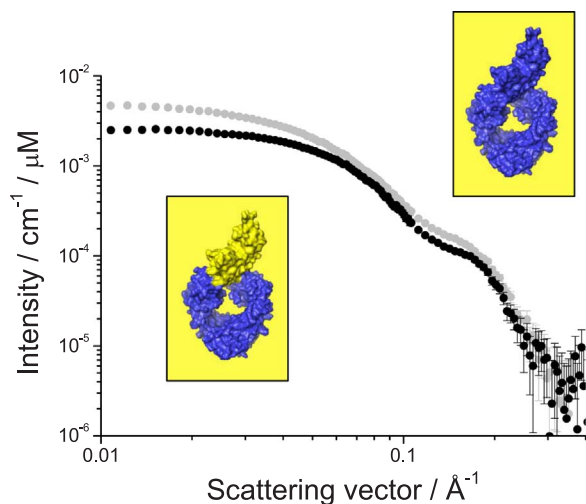


Fig. 3. SANS profiles for Fc in the presence of non-deuterated sFcγRIIIb (gray circles) and Fc in the presence of 75%-deuterated sFcγRIIIb (black circles) in 99.8% D<sub>2</sub>O. Graphical models illustrate deuteration (colored yellow) of solvent and protein based on the crystal structure of the Fc-sFcγRIIIb complex (PDB code 1T89).

sFcγRIIIb. For selective observation of SANS originating from the Fc glycoprotein, we prepared bacterially expressed sFcγRIIIb with 75% deuteration. This sFcγRIIIb preparation was subjected to SANS as well as SAXS in 99.8% D<sub>2</sub>O solution (Fig. S2). The results confirmed that the SANS of 75%-deuterated sFcγRIIIb was matched out with the D<sub>2</sub>O solvent. The SANS profile of IgG1-Fc in complex with 75%-deuterated sFcγRIIIb was significantly different from that observed for Fc-sFcγRIIIb complex without deuteration, demonstrating the successful elimination of SANS contribution of sFcγRIIIb (Fig. 3).

The inversely contrast-matched profile, which originated selectively from the Fc part in the complex, exhibited marked deviation from the profile of IgG1-Fc alone in the high-angle region, although their *R<sub>g</sub>* values calculated from Guinier plots were almost identical, i.e.  $26.3 \pm 0.4 \text{ \AA}$  and  $26.5 \pm 0.3 \text{ \AA}$  for Fc in the presence and absence of 75%-deuterated sFcγRIIIb, respectively (Fig. S3 and Table S3). This indicates that Fc undergoes subtle conformational rearrangement upon binding to sFcγRIIIb in solution, presumably as indicated by the crystallographic data (Fig. 1). Because the scattering curve in the *q*-range of  $0.12\text{--}0.2 \text{ \AA}^{-1}$  sensitively reflects the structural perturbations on the horseshoe-shape of IgG1-Fc (*vide supra*), the quaternary structural change induced by sFcγRIIIb binding is expected to affect SANS profile in this range. Hence, we compared the observed SANS profile of Fc complexed with 75%-deuterated sFcγRIIIb with the profile simulated from the Fc part of the previously reported crystal structure of the Fc-

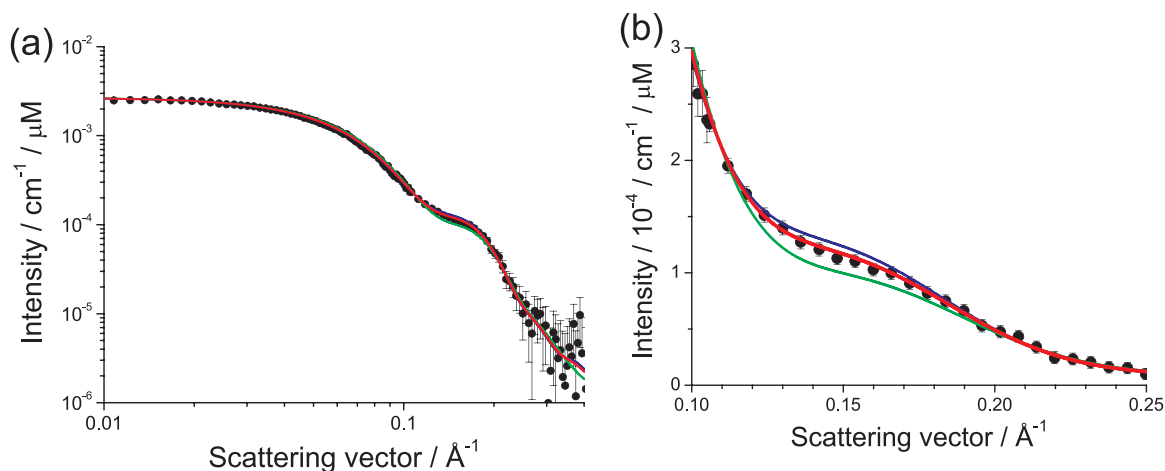


Fig. 4. (a) SANS profile for Fc in complex with 75%-deuterated sFcγRIIIb (closed circles) shown with theoretical profiles computed from the crystal structures of human IgG1-Fc in an uncomplexed state green, and in a sFcγRIIIb-bound state blue. The theoretical profile of 72% sFcγRIIIb-bound form of Fc was reconstructed from the crystal structures of human IgG1-Fc in the free and the sFcγRIIIb-bound forms (red). (b) The enlarged view of (a).

sFc $\gamma$ RIIIb complex [14,15]. The simulated curve is closer to the experimentally observed profile than that of free Fc, but still exhibits significant deviation from the contrast-matched SANS profile of the complex (Fig. 4).

Because the interaction between human IgG1-Fc and sFc $\gamma$ RIIIb is characterized by their low affinity, the remaining discrepancy might be attributed to partial dissociation of the complex. Taking into account the possible partial dissociation of the complex, the residual sum of squares (RSS) between the experimental and simulated data was calculated for varying ratios of sFc $\gamma$ RIIIb-bound Fc (Fig. S4). The RSS plotted as a function of the bound Fc ratio exhibited a minimum of 72% sFc $\gamma$ RIIIb-bound form of Fc. Indeed, the simulated curve computed taking into account this equilibrium was in excellent agreement with the experimentally observed SANS profile (Fig. 4). Because the dissociation constant of the Fc-sFc $\gamma$ RIIIb interaction has been reported to be  $1.4 \times 10^{-6}$  M [16], the mixture of Fc and sFc $\gamma$ RIIIb subjected to the SANS measurement (at each concentration of 16  $\mu$ M) is supposed to be under equilibrium between 26% free and 74% sFc $\gamma$ RIIIb-bound form. Thus, the partial dissociation of the low-affinity protein complex could be successfully treated in this approach.

The present study demonstrated the utility of the SANS approach with inverse contrast-matching technique for structural characterization of a protein with glycosylation that undergoes conformational rearrangement upon formation of a weakly associated biomolecular complex. This is because the use of approximately 100% D<sub>2</sub>O as solvent for inverse matching enables us to obtain high S/N data even in the higher  $q$ -range. Thus, the deuteration-assisted SANS method plays a key role in the integrative structural biology approach to deal with complicated biomacromolecular complexes composed of weakly associated building blocks with conformational plasticity.

#### Acknowledgements

We thank Dr. Susumu Uchiyama (Osaka University) for useful discussion. This work was supported by grants (JP16H00766 and JP15H02042 to M.S., and JP25102001, JP25102008, JP15K21708, and JP15H02491 to K.K., and JP17H05893 to S. Y.) from the Ministry of Education, Culture, Sports, Science and Technology (MEXT) of Japan, by the Okazaki ORION project, and by the Joint Studies Program in the Okazaki BIO-NEXT project of the Okazaki Institute for Integrative Bioscience. The SANS experiments at ILL were performed under proposal No. 8-03-884 and the SAXS experiments at BL15A2 were also performed under proposal No. 2015G658.

#### Appendix A. Transparency document

Supplementary data associated with this article can be found in the

online version at <http://dx.doi.org/10.1016/j.bbrep.2017.08.004>.

#### References

- [1] A. Sali, H.M. Berman, T. Schwede, J. Trehwella, G. Klewegt, et al., Outcome of the first wwPDB hybrid/integrative methods task force workshop, *Structure* 23 (2015) 1156–1167.
- [2] J. Feigon, H. Chan, J. Jiang, Integrative structural biology of Tetrahymena telomerase - insights into catalytic mechanism and interaction at telomeres, *FEBS J.* 283 (2016) 2044–2050.
- [3] J.R. Perilla, G. Zhao, M. Lu, J. Ning, G. Hou, et al., CryoEM Structure Refinement by Integrating NMR Chemical Shifts with Molecular Dynamics Simulations, *J. Phys. Chem. B* (2017).
- [4] D.M. Engelman, P.B. Moore, B.P. Schoenborn, Neutron scattering measurements of separation and shape of proteins in 30S ribosomal subunit of Escherichia coli: S2-S5, S5-S8, S3-S7, *Proc. Natl. Acad. Sci. USA* 72 (1975) 3888–3892.
- [5] H.H. Niemann, M.V. Petoukhov, M. Härtlein, M. Moulin, E. Gherardi, et al., X-ray and neutron small-angle scattering analysis of the complex formed by the Met receptor and the Listeria monocytogenes invasion protein InlB, *J. Mol. Biol.* 377 (2008) 489–500.
- [6] M. Sugiyama, H. Sahashi, E. Kurimoto, S. Takata, H. Yagi, et al., Spatial arrangement and functional role of alpha subunits of proteasome activator PA28 in hetero-oligomeric form, *Biochem. Biophys. Res. Commun.* 432 (2013) 141–145.
- [7] M. Sugiyama, H. Yagi, T. Yamaguchi, K. Kumoi, M. Hirai, et al., Conformational characterization of a protein complex involving intrinsically disordered protein by small-angle neutron scattering using the inverse contrast matching method: a case study of interaction between alpha-synuclein and PbaB tetramer as a model chaperone, *J. Appl. Crystallogr.* 47 (2014) 430–435.
- [8] Z. Ibrahim, A. Martel, M. Moulin, H.S. Kim, M. Härtlein, et al., Time-resolved neutron scattering provides new insight into protein substrate processing by a AAA + unfoldase, *Sci. Rep.* 7 (2017) 40948.
- [9] M. Sugiyama, H. Yagi, K. Ishii, L. Porcar, A. Martel, et al., Structural characterization of the circadian clock protein complex composed of KaiB and KaiC by inverse contrast-matching small-angle neutron scattering, *Sci. Rep.* 6 (2016) 35567.
- [10] A. Appolaire, E. Girard, M. Colombo, M.A. Dura, M. Moulin, et al., Small-angle neutron scattering reveals the assembly mode and oligomeric architecture of TET, a large, dodecameric aminopeptidase, *Acta Crystallogr. D: Biol. Crystallogr.* 70 (2014) 2983–2993.
- [11] L.G. Trabuco, E. Villa, K. Mitra, J. Frank, K. Schulten, Flexible fitting of atomic structures into electron microscopy maps using molecular dynamics, *Structure* 16 (2008) 673–683.
- [12] A. Singharoy, I. Teo, R. McGreevy, J.E. Stone, J. Zhao, et al., Molecular dynamics-based refinement and validation for sub-5 Å cryo-electron microscopy maps, *Elife* (2016) 5.
- [13] R.F. Collins, V. Kargas, B.R. Clarke, C.A. Siebert, D.K. Clare, et al., Oligomeric structure of Wzz determined by cryoelectron microscopy reveals insights into membrane-bound states, *Structure* 25 (2017) (806-+) (Full-length).
- [14] S. Matsumiya, Y. Yamaguchi, J. Saito, M. Nagano, H. Sasakawa, et al., Structural comparison of fucosylated and nonfucosylated Fc fragments of human immunoglobulin G1, *J. Mol. Biol.* 368 (2007) 767–779.
- [15] S. Radaev, S. Motyka, W.H. Fridman, C. Sautes-Fridman, P.D. Sun, The structure of a human type III Fc $\gamma$  receptor in complex with Fc, *J. Biol. Chem.* 276 (2001) 16469–16477.
- [16] K. Maenaka, P.A. van der Merwe, D.I. Stuart, E.Y. Jones, P. Sondermann, The human low affinity Fc $\gamma$  receptors IIa, IIb, and III bind IgG with fast kinetics and distinct thermodynamic properties, *J. Biol. Chem.* 276 (2001) 44898–44904.